IEEE Access
Multidisciplinary | Rapid Review | Open Access Journal

Received May 8, 2022, accepted May 21, 2022, date of publication May 25, 2022, date of current version June 3, 2022.

Digital Object Identifier 10.1109/ACCESS.2022.3177838

Robust Localization Based on Mixed-Norm Minimization Criterion

CHEE-HYUN PARK AND JOON-HYUK CHANG, (Senior Member, IEEE)
School of Electronics Engineering, Hanyang University, Seoul 133-791, South Korea

Corresponding author: Joon-Hyuk Chang (jchang@hanyang.ac.kr)

This work was supported by the Institute of Information Communications Technology Planning Evaluation (IITP) Grant funded by the Korea Government [Ministry of Science and Information Communications Technology (MSIT)] (Development of Ultra-High Speech Quality Technology for Remote Multi-Speaker Conference System) under Grant 2021-0-00456.

ABSTRACT This paper presents robust positioning methods that use range measurements to estimate location parameters. The existing maximum correntropy criterion-based localization algorithm uses only the l_2 norm minimization. Therefore, the localization performance may not be satisfying because the l_2 norm minimization is vulnerable to the large error. Therefore, we propose the convex combination of l_1 and l_2 norm because the l_1 norm minimization is effective in the large noise condition. The mixed-norm maximum Versoria criterion-based unscented Kalman filter, mixed-norm least lncosh unscented Kalman filter, mixed-norm maximum Versoria criterion iterative reweighted least-squares, mixed-norm least lncosh iterative reweighted least squares and closed-form localization approaches are proposed for mixed line-of-sight/non-line-of-sight environments. The proposed mixed-norm unscented Kalman filter-based algorithms are more superior to the other methods as the line-of-sight noise level increases by the use of the convex combination of l_1 norm and l_2 norm. The iterative reweighted least sqaures-based methods employ a weight matrix. The closed-form weighted least squares algorithm has an advantage that its computational complexity is lower than that of other methods. Simulation and experiments illustrate the localization accuracies of the proposed unscented Kalman filter-based methods are found to be superior to those of the other algorithms under large noise level conditions.

INDEX TERMS Digital signal processing, distributed information systems, filtering theory, indoor navigation, iterative algorithms, location awareness, mobile communication, parameter estimation, radio navigation, robustness.

I. INTRODUCTION

In emitter positioning, the coordinates of the source are predicted by utilizing the measurements of each sensor, which include the time difference of arrival, time of arrival (TOA), received signal strength, and angle of arrival. Point target positioning is crucial in various research areas such as mobile communications, telecommunications, radar and sonar. Blocking or obstruction does not exist in line-of-sight (LOS) situations. However, the LOS path between the source and sensors may be obstructed in indoor and urban settings. An outlier is defined as data that significantly differs from other most clustered observations. When an outlier exists in TOA localization, the time delay may be significantly larger than the actual delay owing to the positively biased multipath; thus, the localization performance can be severely degraded when using this false time delay. The goal of this study is to provide a method for estimating location parameters robustly against the outlier-contaminated non-LOS (NLOS) noise.

The associate editor coordinating the review of this manuscript and approving it for publication was Gerard-Andre Capolino.

A. RELATED WORK

Substantial studies have been conducted on localization problems under LOS conditions [1]–[6]. However, despite recent studies on positioning in NLOS environments, there are relatively few investigations for the localization in the NLOS environments. Location estimation under NLOS conditions has been researched; for example, 1) mathematical optimization [7]–[11], 2) robust statistics [12]–[18], 3) LOS and NLOS sensor identification [19]–[21] and 4) robust adaptive filter, extended Kalman filter (EKF) or unscented Kalman filter (UKF) [22]–[28]. The localization algorithm using multiple heterogeneous devices has been proposed [29].

This method makes more realistic assumption that users have different kinds of devices. The positioning algorithm employing the compartment model is proposed [30]. The computational complexity is low because mini-batch singular value decomposition method is used. However, it requires the training-step and noise statistics. They should be adapted again when the environment is changed. Also, the divergence problem may exist because it is an iteration-based algorithm. Furthermore, the target detection algorithm is just suboptimal because it is not based on the likelihood-ratio testing. Also, the positioning algorithm in which Huber M estimation and particle filter are combined is investigated [31]. However, the computational complexity would be intensive because they use the particle filtering. In [32], the self-training procedure based localization has been proposed where the requirement of labeled data is avoided and the self-training procedure does not need to train additional learners. The localization and synchronization (LAS) techniques are developed using the doppler and TOA measurements [33]. The LAS problem is formulated as a maximum likelihood (ML) problem and the optimal solution is calculated iteratively. The localization methods in which received signal strength (RSS) and TOA measurements are fused are developed [34]–[36] to overcome mixed LOS/NLOS problems. However, the accuracy of RSS-based systems is known to be inferior to the other positioning methods such as time delay techniques. Also, the channel parameters such as transmitted signal power and pathloss exponent cannot be obtained conveniently. The distribution of the path length (i.e., absolute time delay) of the first-arriving multipath component (MPC) is derived. This result is then used to attain the NLOS bias distribution. This distribution is shown to match well with previously assumed gamma and exponential NLOS bias models [37]. The Kalman filter has been widely used in localization and tracking, but its positioning performance is severely degraded in the presence of outliers. The Kalman filter is employed twice for mitigating the NLOS error and estimating the location and the identification step is incorporated into the algorithm to overcome the weakness of Kalman filter in NLOS contaminated situation [38]. Recently, the maximum correntropy criterion (MCC) has received wide attention as an outlier-resistant technique [22], [23]. Robust Kalman filters, such as MCC-EKF and MCC-UKF, demonstrate superior performance to those of the conventional Kalman and UKFs under mixed LOS/NLOS conditions [22], [23]. However, the performance of the MCC-based algorithm is unstable and may diverge when a small kernel bandwidth is selected because the exponential Gaussian kernel function is used. Meanwhile, the MVC-based robust algorithm is not susceptible to the weakness of the MCC-based method [39]–[41]. Accordingly, authors consider the MVC-based algorithm for attenuating the adverse effects caused by NLOS measurements. Specifically, the performance of MVC-based robust algorithms can be improved at a large noise level by exploiting a convex combination of the Versoria functions with l_1 and l_2 norms.

The reason why the convex combination of Versoria functions is employed as the cost function is as follows: The l_1 norm minimization is robust to large amplitude noise or anomalies compared to the l_2 norm minimization [42], [43]. In general, when the heavy-tailed noise does not exist or noise level is relatively low, the l_2 norm minimization method provides less misadjustment than l_1 norm minimization [42], [43]. With each advantage of the l_1 norm and l_2 norm, the enhancement of estimation performance is expected in the low signal-to-noise ratio (SNR) regimes where the spurious peaks and impulsive noise occur more frequently, preserving efficiency in the small noise conditions. This mixed-norm minimization can be observed in widely used robust algorithms, such as the M estimator, where the l_2 loss is minimized when the residual is small and l_1 loss is minimized when the residual is large [44]–[46]. The Versoria function has the heavier tail than that of the Student's t distribution with three degrees of freedom. The tail of the Versoria function becomes thicker with the increase of the diameter [45], [46]. Therefore, the Versoria function is suitable for representing heavy-tailed data. The Versoria cost function decreases as the magnitude of error is larger and the solution is determined such that the squared error is minimized. The lncosh cost function increases as the magnitude of error is larger and the solution is determined such that the magnitude of error is minimized. The mixed-norm Versoria function is displayed in Fig. 1(a). Furthermore, the llncosh algorithm behaves like a hybrid of the l_1 and l_2 norm minimization methods; its cost function is shown in Fig. 1(b). However, the llncosh algorithm utilizes the least mean squares (LMS) or affine projection LMS method to minimize the cost function. Therefore, although the computational burden may be low, the convergence rate may be slow and the misadjustment is relatively large compared to other optimal statistical algorithms. Hence, the iterative reweighted least-squares (IRLS) method is used to improve the accuracy of the LMS-based llncosh methods by introducing a weight matrix. The weight matrix is constructed as the inverse of the noise variance; however, the transformed observation variance of the NLOS sensor is generally unknown because the noise variance of an NLOS transformed measurement depends on the unknown measurement bias and NLOS noise variance. To circumvent this problem, the variance of the NLOS transformed observation is estimated using the squared residual between the transformed observation and least median of squares (LMedS) estimate of transformed range. This noise variance estimation algorithm was developed inspired by the existing residual weighting (RWGH) method [47]. The weight is smaller as the noise variance increases and vice versa. Meanwhile, as in various existing studies, we assume that the noise variance of the LOS observation (inlier) is known *a priori*. The aforementioned localization methods are iteration-based algorithms. They require an initial guess solution and may diverge in some adverse situations. Therefore, the closed-form localization method is developed, where the LMedS solution is used to

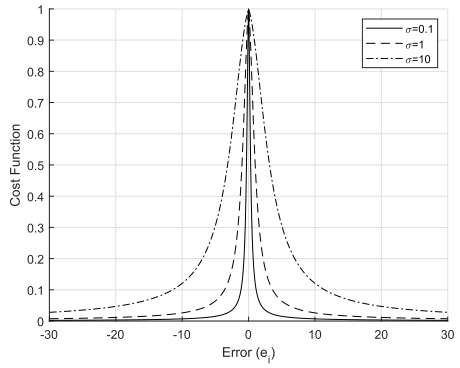

(a)

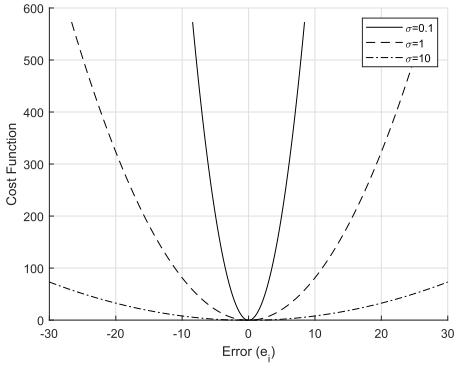

(b)

FIGURE 1. Cost function as a function of error for different σ (a) Mixed-norm Versoria function (α: mixing constant=0.8, σ: kernel bandwidth) (b) Mixed-norm lncosh function (α =0.8).

construct the weight matrix based on the RWGH method [47] and the final solution is obtained using the well-known two-step weighted least squares (WLS) method [2].

B. CONTRIBUTIONS

The main contributions can be summarized as follows:

- Robust UKF localization methods are developed, where the l_1/l_2 mixed-norm MVC is adopted for estimating the location parameter. Note that the mixed-norm MVC has not yet been investigated in the existing literatures.
- The mixed-norm MVC IRLS and llncosh IRLS (LLIRLS)-based methods are developed, for which the weight matrix is adopted. In general, Versoria function maximization is performed via the LMS or affine projection LMS method without the weight matrix. The estimation performance of the LMS-based methods is improved by using a weight matrix. To the best of authors' knowledge, our study using the weight matrix in the MVC is the first case.
- The approximate variance of the NLOS transformed observation is obtained via the squared residual. The LMedS solution is obtained in advance and the variance is approximated as the squared residual. With this weight matrix, IRLS and closed-form solutions are obtained.

The l_2 norm minimization is weak to the environment in which the noise level is large or heavy-tailed noise exists. Meanwhile, the l_1 norm minimization is robust against the spurious peaks and impulsive noise which occur more frequently as the noise level increases. Therefore, the mixed-norm (combination of the l_1/l_2 norm) strategy is more effective. Namely, the mixed-norm algorithm is advantageous in the large noise level or heavy-tailed noise condition. However, the disadvantage of the mixed-norm UKF-based algorithms is that it has a heavy computational complexity and requires the appropriate selection of mixing constant. Also, the IRLS-based methods have advantage in the low noise condition because it has been designed ignoring the second-order noise term. Furthermore, the computational burden of the closed-form WLS method is lower than those of other algorithms, thus it may be utilized in real-time scenarios. The MVC and llncosh rules have been studied in existing literature [24], [39]–[41]. However, to the best of our knowledge, mixed-norm MVC and mixed-norm llncosh methods have not yet been investigated in the existing literature.

C. ORGANIZATION

This paper is organized as follows. Section II addresses the mixed LOS/NLOS location estimation problem. Section III briefly introduces existing methods. Section IV describes the proposed robust localization methods, that is, the mixed-norm MVC UKF, mixed-norm llncosh UKF (LLUKF), mixed-norm MVC IRLS, mixed-norm LLIRLS and closed-form methods. Sections V and VI evaluate the root mean square error (RMSE) performance based on the simulation and experimental results. Finally, Section VII presents the conclusions. In addition, notations used in this paper are described for readability in the Table 1.

II. PROBLEM FORMULATION

The objective of the range-based emitter localization method is to accurately predict the location of a point-target using range measurements, to minimize the error criterion, i.e., the MSE, the sum of the squared error or the mean absolute error. The measurement equation in the context of the source positioning under mixed LOS/NLOS conditions is represented as

$$r_i = d_i + n_i = \sqrt{(q_1 - x_i)^2 + (q_2 - y_i)^2} + n_i, \qquad (1)$$

where n_i is distributed by $N(0, \sigma_1^2)\mathbb{1}\{r_i \in L\} + N(\mu_2, \sigma_2^2)$ $\mathbb{1}\{r_i \in L^c\}$, $i = 1, 2, \ldots, M$ with M denoting the total number of sensors, L is the sensor set which is in the LOS state and L^c is the NLOS sensor set, respectively [48]–[51]. Additionally, $\mathbb{1}\{\cdot\}$ is an indicator function. The indicator function represents a random variable for an event that equals 1 when the event occurs and zero when the event does not occur. The measurement error n_i is a random variable that follows a Gaussian distribution with $N(0,\sigma_1^2)$ when the corresponding sensor belongs to the LOS sensor

TABLE 1. Notation description.

Notation	Description
r_i	distance measurement between the source and the i^{th} sensor
d_i	true distance between the source and the i^{th} sensor
n_i	weighted sum of LOS and NLOS noise of the i^{th} sensor
m_i	noise of the transformed distance measurement of the i^{th} sensor
$N(\mu, \sigma^2)$	normal distribution in which the mean is μ and the variance is σ^2
σ_1^2	variance of the LOS noise
σ_2^2	variance of the NLOS noise
μ_2	bias of the NLOS noise
L	LOS sensor set
L^c	NLOS sensor set
x_i	x-axis coordinate of the i^{th} sensor
y_i	y-axis coordinate of the i^{th} sensor
q_i	i^{th} true coordinate of the source
q_3	$q_1^2 + q_2^2$
b_i	transformed distance measurement of the i^{th} sensor
V	Versoria function
D	diameter of the generating adjoined circle of the Versoria function
τ	Versoria shape parameter
e	estimation error of the estimator
$\aleph$	sigma point
$\mathbf{P}_{k\|k-1}$	state prediction error covariance matrix
$\mathbf{P}_{k\|k}$	state estimation error covariance matrix
$\mathbf{R}$	measurement error covariance matrix
$\mathbf{A}$	design matrix
$\mathbf{b}$	transformed measurement vector
$\mathbf{W}$	weight matrix
α	mixing constant
$\mathbf{K}_k$	Kalman gain in the k^{th} time step
$\mathbb{1}$	indicator function
$\mathbf{q}_k$	state vector
$\hat{\mathbf{q}}_{k\|k-1}$	prediction state vector
$\hat{\mathbf{q}}_{k\|k}$	estimation state vector
$\sigma_{b_i}^2$	variance of the i^{th} transformed measurement
V_{mixed}	mixed-norm Versoria function
C_{mixed}	mixed-norm lncosh function

set (L), whereas follows $N(\mu_2,\sigma_2^2)$ when it belongs to the NLOS set (L^c). In general, whether the sensor is in the LOS or NLOS state cannot be known *a priori* in most cases; thus, the state of the sensor is predicted via statistical testing [52]. In addition, the mean and variance of the outlier distribution cannot be obtained. Furthermore, $[q_1, q_2]^T$ represents the unknown emitter coordinates and $[x_i, y_i]^T$ represents the known coordinates of the i^{th} receiver. Moreover, r_i is the distance observation between the point emitter and the i^{th} sensor and d_i is the true range between the emitter and the i^{th} receiver. Squaring (1) and rearranging yield the following equation:

$$x_i q_1 + y_i q_2 - 0.5 q_3 + m_i = 0.5(x_i^2 + y_i^2 - r_i^2), \ \ i = 1, 2, \ldots, M, \tag{2}$$

where $q_3 = q_1^2 + q_2^2$, $m_i = -d_i n_i - \frac{1}{2} n_i^2$. By representing (2) in a matrix form, we obtain the following

$$\mathbf{A}\mathbf{q} + \mathbf{m} = \mathbf{b}, \tag{3}$$

where $\mathbf{m} = [m_1, \cdots, m_M]^T$, $\mathbf{q} = [q_1, q_2, q_3]^T$,

$$\mathbf{A} = \begin{pmatrix} x_1 & y_1 & -0.5 \\ \vdots & \vdots & \vdots \\ x_M & y_M & -0.5 \end{pmatrix},$$

$$\text{and} \ \ \mathbf{b} = [b_1, \cdots, b_M]^T = \frac{1}{2} \begin{pmatrix} x_1^2 + y_1^2 - r_1^2 \\ \vdots \\ x_M^2 + y_M^2 - r_M^2 \end{pmatrix}.$$

It should be noted that the proposed algorithms utilize a single sample different from the previous study of the authors [41],

[53]; its computational complexity may be lower than those of multiple measurement-based methods. In this study, a vector and a matrix are denoted by a lowercase and an uppercase boldface letters, respectively, and the operator $[\cdot]^T$ denotes a vector/matrix transpose.

Remark 1: Recently, the Kalman filter approach for estimating simultaneously the source location and measurement bias has been investigated, but the accuracy is not satisfactory. In addition, the measurement bias is regarded as a constant in this study, not through the entire period but for estimation interval. Namely, the measurement bias may be different for each estimation period.

III. PRELIMINARIES

Adaptive filters with the MVC and llncosh criterion have been employed in the presence of outliers [24], [39], [40]. In addition, the Kalman filter with the MVC has been proposed in the context of multiple observations [34]. The rationale of adaptive filter and Kalman filtering exploiting the MVC is to employ the Versoria function, where the Versoria function decreases as the magnitude of the residual increases and vice versa. The essence of the llncosh-based adaptive filter and Kalman filtering is to minimize the lncosh function, where the lncosh function decreases as the magnitude of the residual decreases and vice versa. The standard Kalman filter cannot be directly used because the range observation in the TOA-based localization is nonlinear with respect to the parameter to be estimated. Therefore, nonlinear Kalman filters, such as the EKF or UKF, must be exploited. The MCC-based and MVC-based EKF and UKF have been investigated in previous studies [22], [23], [41]. However, mixed-norm MVC-based UKF has not been investigated. Hence, the mixed-norm MVC-based UKF is considered in this study. The LMedS estimator has been used as the robust estimation method. Because the accuracy of LMedS algorithm is inferior to the other robust methods, it is used to obtain the initial estimate of more complex and accurate robust algorithms.

A. LMedS ESTIMATOR [12]–[14]

The LMedS method estimates the location parameters by solving the following:

$$\min \text{med}_i \ \ e_i^2, \quad i = 1, \cdots, K \tag{4}$$

where e_i^2 is the squared residual, $K = \binom{M}{p}$ (binomial coefficient) and p denotes the number of elements of the subset, respectively. The LMedS algorithm is used to determine the initial point of the follow-up robust localization method.

B. VERSORIA FUNCTION

The original Versoria function is represented as follows [39], [40]:

$$V(e_i) = \frac{D^3}{D^2 + e_i^2} = \frac{2a}{1 + \tau e_i^2} \tag{5}$$

where e_i is the residual defined as $e_i = r_i - \hat{d}_i$, $\hat{d}_i$ is the range estimate of the ith sensor, $D = 2a$ is the diameter of the generating adjoined circle of the Versoria function and $\tau = (1/2a)^2$ is the Versoria shape parameter. The following loss function is employed to obtain a robust solution [39]–[41]:

$$V(e_i) = \frac{\sigma_i}{1 + (\frac{e_i}{\sigma_i})^2} \propto \frac{1}{1 + (\frac{e_i}{\sigma_i})^2}, \quad i = 1, \cdots, M. \tag{6}$$

Note that the l_2 norm in the denominator of the Versoria function ($V(e_i)$). The estimation accuracy of l_2 norm minimization is severely degraded under large noise conditions, where spurious peaks and impulsive noise occur more frequently. Therefore, the conventional Versoria function should be modified by employing the convex combination of l_1 and l_2 Versoria functions.

C. EXISTING MVC UKF [23], [41], [54]

The UKF algorithm can be used in the highly nonlinear and non-differentiable systems, improving the estimation accuracy. The unscented transform is adopted in the Kalman filter recursion and this is known as the UKF [55], [56]. The state and measurement models exploited in this study are represented as follows:

$$\mathbf{q}_k = \mathbf{q}_{k-1} \tag{7}$$

$$\mathbf{r}_k = \mathbf{h}(\mathbf{q}_k) + \mathbf{n}_k \tag{8}$$

where $\mathbf{q}_k$ is the state vector in the k^{th} time step, $\mathbf{h}(\cdot)$ is the nonlinear Euclidean distance function and $\mathbf{n}_k = [n_{1,k} \cdots n_{M,k}]^T$ is the observation noise vector in the k^{th} time step. Unless otherwise stated, (7) and (8) are used as the state and measurement equations throughout the remainder of the paper. The existing MVC UKF employs the Versoria function instead of the Gaussian kernel function of the MCC UKF. The existing MVC UKF is summarized in Algorithm 1.

IV. PROPOSED ROBUST ALGORITHMS

In this section, the proposed robust algorithms are presented. The l_1 norm minimization is more effective than l_2 norm minimization when outliers exist. Meanwhile, the l_2 minimization is better than the l_1 norm minimization in the LOS situation. Therefore, the estimation performance of the proposed methods would be degraded when the l_1 norm minimization is overly emphasized in the lightly outlier-contaminated environment or LOS situation. Accordingly, the proposed methods utilize the appropriate combination of l_1/l_2 norm minimization to tackle the heavy-tailed noise. Also, the weight is employed in the IRLS-based methods and closed-form algorithm to outperform non-weighted algorithms. The weight is larger as the noise variance is smaller and vice versa.

A. THE MIXED NORM-BASED MVC UKF

The l_1/l_2 mixed-norm-based MVC UKF is investigated to improve the accuracy of l_2 norm-based MVC UKF in the large noise level. The mixed norm-based MVC UKF is

Algorithm 1 Existing MVC-Based UKF

Initialize the state vector, $\hat{\mathbf{q}}_{0|0}$ and the covariance matrix, $\mathbf{P}_{0|0}$

1. Calculate the prediction sigma points

$\aleph_{0,k-1|k-1} = \hat{\mathbf{q}}_{k-1|k-1}$

$\aleph_{s,k-1|k-1} = \hat{\mathbf{q}}_{k-1|k-1} + [\sqrt{(n+\lambda)\mathbf{P}_{k-1|k-1}}]_s$, $s = 1, \cdots, n$

$\aleph_{s,k-1|k-1} = \hat{\mathbf{q}}_{k-1|k-1} - [\sqrt{(n+\lambda)\mathbf{P}_{k-1|k-1}}]_s$, $s = n+1, \cdots, 2n$

where $[\sqrt{(n+\lambda)\mathbf{P}_{k-1|k-1}}]_s$ is the s^{th} column of $\sqrt{(n+\lambda)\mathbf{P}_{k-1|k-1}}$, $\hat{\mathbf{q}}_{k-1|k-1}$ is the state estimation at time index $k-1$, $\mathbf{P}_{k-1|k-1}$ is the error covariance matrix at time index $k-1$ and λ is a tuning parameter.

2. Propagate the sigma points through the nonlinear process model $\aleph^*_{s,k-1|k-1} = \aleph_{s,k-1|k-1}, \quad s = 0, \cdots, 2n$.

3. Obtain predicted state and covariance:

$\hat{\mathbf{q}}_{k|k-1} = \sum_{s=0}^{2n} W_s^q \aleph^*_{s,k|k-1}$

$\mathbf{P}_{k|k-1} = \sum_{s=0}^{2n} W_s^P (\aleph^*_{s,k|k-1} - \hat{\mathbf{q}}_{k|k-1})(\aleph^*_{s,k|k-1} - \hat{\mathbf{q}}_{k|k-1})^T$

where the definitions of W_s^q and W_s^P can be found in [23] and [55].

4. Calculate the update sigma points

5. Propagate the sigma points through the nonlinear measurement model

$\mathbf{r}_{s,k|k-1} = h(\aleph_{s,k|k-1}), \quad s = 0, \cdots, 2n$

6. Calculate the predicted measurement, covariance and cross covariance matrices

$\hat{\mathbf{r}}_{k|k-1} = \sum_{s=0}^{2n} W_s^q \mathbf{r}_{s,k|k-1}$

$\mathbf{P}_{rr,k|k-1} = \sum_{s=0}^{2n} W_s^P (\mathbf{r}_{s,k|k-1} - \hat{\mathbf{r}}_{k|k-1})(\mathbf{r}_{s,k|k-1} - \hat{\mathbf{r}}_{k|k-1})^T + \mathbf{R}_k$

$\mathbf{P}_{qr,k|k-1} = \sum_{s=0}^{2n} W_s^P (\aleph_{s,k|k-1} - \hat{\mathbf{q}}_{k|k-1})(\mathbf{r}_{s,k|k-1} - \hat{\mathbf{r}}_{k|k-1})^T$

where $\mathbf{R}_k$ denotes the measurement error covariance matrix.

7. Calculate the pseudo measurement matrix

$\bar{\mathbf{H}}_k = \mathbf{P}^T_{qr,k|k-1} \mathbf{P}^{-1}_{rr,k|k-1}$.

8. Calculate the modified $\bar{\mathbf{P}}_{k|k-1}$ and $\bar{\mathbf{R}}_k$

$\mathbf{D}_k = \begin{bmatrix} \hat{\mathbf{q}}_{k|k-1} \\ \mathbf{r}_k - \hat{\mathbf{r}}_{k|k-1} + \bar{\mathbf{H}}_k \hat{\mathbf{q}}_{k|k-1} \end{bmatrix}$, $\mathbf{W}_k = \begin{bmatrix} \mathbf{I} \\ \bar{\mathbf{H}}_k \end{bmatrix}$,

$\mathbf{e}_k = \mathbf{D}_k - \mathbf{W}_k \hat{\mathbf{q}}_{k-1|k-1}$, $\mathbf{V}_{q,k} = \text{diag}(V(e_{1,k}), \cdots, V(e_{n,k}))$, $\mathbf{V}_{r,k} = \text{diag}(V(e_{n+1,k}), \cdots, V(e_{n+M,k}))$

where $e_{l,k} = \hat{q}_{l,k|k-1} - \hat{q}_{l,k-1|k-1}$ $(l=1,\cdots,n)$, $\hat{q}_{l,k|k-1}$ is the l^{th} component of $\hat{\mathbf{q}}_{k|k-1}$, $e_{n+i,k} = r_i - \hat{r}_{i,k|k-1} - \bar{\mathbf{h}}^T_{i,k}(\hat{\mathbf{q}}_{k|k-1} - \hat{\mathbf{q}}_{k-1|k-1})$ $(i=1,\cdots,M)$, $\bar{\mathbf{h}}^T_{i,k}$ is the i^{th} row of $\bar{\mathbf{H}}_k$, $\hat{r}_{i,k|k-1}$ is the i^{th} component of $\hat{\mathbf{r}}_{k|k-1}$, $V(e_{l,k})$ is the Versoria function defined as $\frac{1}{1+(\frac{e_{l,k}}{\sqrt{\mathbf{P}_{k|k-1}(j,j)}})^2}$ $(l=1,\cdots,n)$, $\frac{1}{1+(\frac{e_{l,k}}{\sigma_1})^2}$ $(l=n+1,\cdots,n+M)$ and $\mathbf{P}_{k|k-1}(j,j)$ is the j^{th} diagonal component of $\mathbf{P}_{k|k-1}$

$\bar{\mathbf{P}}_{k|k-1} = \mathbf{V}^{-1}_{q,k}$, $\bar{\mathbf{R}}_k = \mathbf{V}^{-1}_{r,k}$

9.Update mean and error covariance

$\hat{\mathbf{q}}_{k|k} = \hat{\mathbf{q}}_{k|k-1} + \bar{\mathbf{K}}_k(\mathbf{r}_k - \hat{\mathbf{r}}_{k|k-1})$

$\mathbf{P}_{k|k} = (\mathbf{I} - \bar{\mathbf{K}}_k \bar{\mathbf{H}}_k)\mathbf{P}_{k|k-1}(\mathbf{I} - \bar{\mathbf{K}}_k \bar{\mathbf{H}}_k)^T + \bar{\mathbf{K}}_k \mathbf{R}_k \bar{\mathbf{K}}_k$

where $\bar{\mathbf{K}}_k = \bar{\mathbf{P}}_{k|k-1} \bar{\mathbf{H}}^T_k (\bar{\mathbf{R}}_k + \bar{\mathbf{H}}_k \bar{\mathbf{P}}_{k|k-1} \bar{\mathbf{H}}_k)^{-1}$

similar to the existing MVC UKF, except that the mixed-norm-based Versoria function is exploited instead of the l_2-norm Versoria function. Note that statistical testing, with which the LOS or NLOS state of the sensor is predicted, is not required in the UKF-based method. This is the advantage of the UKF-based method compared to the IRLS-based algorithm and closed-form method, which require statistical testing. Subsequently, the mixed norm-based MVC UKF is summarized in Algorithm 2.

Algorithm 2 Mixed Norm-Based MVC UKF

1-7. Identical with Algorithm 1.

8. Utilize the mixed norm-based Versoria function defined as follows:

$\mathbf{V}^q_{\text{mixed}} = \text{diag}[V_{\text{mixed}}(e_{1,k}), \cdots, V_{\text{mixed}}(e_{n,k})]$

where $e_{j,k} = \hat{q}_{j,k|k-1} - \hat{q}_{j,k-1|k-1}$ and $\hat{q}_{j,k|k-1}$ is the j^{th} component of $\hat{\mathbf{q}}_{k|k-1}$.

$V_{\text{mixed}}(e_{j,k}) = \alpha\left(\frac{1}{1+(\frac{e_{j,k}}{\sqrt{\mathbf{P}_{k|k-1}(j,j)}})^2}\right) + (1-\alpha)\left(\frac{1}{1+\frac{|e_{j,k}|}{\sqrt{\mathbf{P}_{k|k-1}(j,j)}}}\right)$, $j=1,\cdots,n$

where $\alpha \in [0, 1]$ is a mixing constant.

$\mathbf{V}^r_{\text{mixed}} = \text{diag}[V_{\text{mixed}}(e_{n+1,k}), \cdots, V_{\text{mixed}}(e_{n+M,k})]$

$V_{\text{mixed}}(e_{n+i,k}) = \alpha\left(\frac{1}{1+(\frac{e_{n+i,k}}{\sigma_1})^2}\right) + (1-\alpha)\left(\frac{1}{1+\frac{|e_{n+i,k}|}{\sigma_1}}\right)$, $i=1,\cdots,M$

where $e_{n+i,k} = r_i - \hat{r}_{i,k|k-1} - \bar{\mathbf{h}}^T_{i,k}(\hat{\mathbf{q}}_{k|k-1} - \hat{\mathbf{q}}_{k-1|k-1})$ and $\hat{r}_{i,k|k-1}$ is the i^{th} component of $\hat{\mathbf{r}}_{k|k-1}$.

$\bar{\mathbf{P}}_{k|k-1} = (\mathbf{V}^q_{\text{mixed}})^{-1}$, $\bar{\mathbf{R}}_k = (\mathbf{V}^r_{\text{mixed}})^{-1}$

9. Identical with Algorithm 1.

B. THE MIXED NORM-BASED MVC IRLS

The mixed norm minimization can be performed using the MVC IRLS method. The cost function is defined as follows:

$$J = \frac{1}{2\sigma^2_{b_i}} e_i^2 \mathbb{1}(b_i \in \text{LOS}) + \left\{1 - \frac{\alpha}{1+(\frac{e_i}{\sigma_{b_i}})^2} - (1-\alpha)(\frac{1}{1+|\frac{e_i}{\sigma_{b_i}}|})\right\} \mathbb{1}(b_i \in \text{NLOS}) \quad (9)$$

where $\sigma^2_{b_i}$ is the variance of transformed measurement b_i, $e_i = b_i - \mathbf{a}_i^T \mathbf{q}$ and $\mathbf{a}_i^T$ is the i^{th} row of $\mathbf{A}$. Differentiating the cost function with respect to $\mathbf{q}$ yields the following:

$$\frac{\partial J}{\partial \mathbf{q}} = \frac{1}{\sigma^2_{b_i}} e_i \mathbf{a}_i \mathbb{1}(b_i \in \text{LOS}) + \left\{\alpha\left(\frac{\frac{2e_i}{\sigma^2_{b_i}}}{(1+(\frac{e_i^2}{\sigma^2_{b_i}}))^2}\right)\mathbf{a}_i + (1-\alpha)\left(\frac{\frac{e_i}{\sigma_{b_i}}}{(1+\frac{|e_i|}{\sigma_{b_i}})^2|e_i|}\right)\mathbf{a}_i\right\} \mathbb{1}(b_i \in \text{NLOS}). \quad (10)$$

Setting the partial derivative to zeros and concatenating each equation yield the following equation:

$$\mathbf{A}^T \mathbf{W}(\mathbf{b} - \mathbf{A}\mathbf{q}) = \mathbf{0} \quad (11)$$

where $\mathbf{W} = \text{diag}[w_1, \cdots, w_M]$, $w_i = \frac{1}{\sigma_{b_i}^2} = \frac{1}{\sigma_1^2 r_i^2}$ if the i^{th} sensor is predicted to be the LOS sensor. Whether the sensor is in the LOS or NLOS state is predicted using the statistical testing [52]. The weight is calculated when the corresponding sensor is predicted to be an NLOS sensor as follows:

$$w_i = \alpha\left(\frac{\frac{2}{\sigma_{b_i}^2}}{(1+(\frac{e_i^2}{\sigma_{b_i}^2}))^2}\right) + (1-\alpha)\left(\frac{\frac{1}{\sigma_{b_i}}}{(1+\frac{|e_i|}{\sigma_{b_i}})^2|e_i|}\right). \quad (12)$$

Clearly, the noise variance of the NLOS transformed observation ($\sigma_{b_i}^2$) depends on the unknown measurement bias (μ_2) and the outlier noise variance (σ_2^2); thus, the $\sigma_{b_i}^2$ of the NLOS observation is estimated as follows:

$$\sigma_{b_i}^2 = E[(b_i - E[b_i])^2] \simeq (b_i - \hat{b}_i)^2 \quad (13)$$

where $\hat{b}_i = \frac{x_i^2+y_i^2-\hat{d}_i^2}{2}$, $\hat{d}_i = \sqrt{(\hat{q}_1 - x_i)^2 + (\hat{q}_2 - y_i)^2}$ and $[\hat{q}_1, \hat{q}_2]^T$ is the estimated position using the LMedS estimate obtained in the first-step. This noise variance estimation approach was adopted in the existing RWGH method [47]. Then, the WLS estimate can be obtained as follows:

$$\hat{\mathbf{q}} = (\mathbf{A}^T\mathbf{W}\mathbf{A})^{-1}\mathbf{A}^T\mathbf{W}\mathbf{b}. \quad (14)$$

Furthermore, the accuracy of the second-step estimate can be improved using the well-known two-step approach [2], [3] and the third-step can be expressed as follows:

$$\hat{\mathbf{q}}_t = (\mathbf{H}^T\mathbf{C}_{\hat{\mathbf{h}}}^{-1}\mathbf{H})^{-1}\mathbf{H}^T\mathbf{C}_{\hat{\mathbf{h}}}^{-1}\hat{\mathbf{h}} \quad (15)$$

where the subscript t denotes the third-step estimate,

$$\hat{\mathbf{h}} = \left[[\hat{\mathbf{q}}]_1^2 \; [\hat{\mathbf{q}}]_2^2 \; [\hat{\mathbf{q}}]_3\right]^T, \quad (16)$$

$$\mathbf{H} = \begin{pmatrix} 1 & 0 \\ 0 & 1 \\ 1 & 1 \end{pmatrix}, \quad (17)$$

$$\mathbf{C}_{\hat{\mathbf{h}}} = \text{diag}[2q_1 \; 2q_2 \; 1](\mathbf{A}^T\mathbf{W}\mathbf{A})^{-1}\text{diag}[2q_1 \; 2q_2 \; 1] \quad (18)$$

$$\simeq \text{diag}[2[\hat{\mathbf{q}}]_1 \; 2[\hat{\mathbf{q}}]_2 \; 1](\mathbf{A}^T\mathbf{W}\mathbf{A})^{-1}\text{diag}[2[\hat{\mathbf{q}}]_1 \; 2[\hat{\mathbf{q}}]_2 \; 1], \quad (19)$$

and $[\hat{\mathbf{q}}]_i$ (i=1,2,3) is the i^{th} component of the second-step estimate. The final emitter position estimate can be expressed as follows:

$$\hat{\mathbf{q}}_e = \left[\text{sgn}([\hat{\mathbf{q}}]_1)\sqrt{[\hat{\mathbf{q}}_t]_1} \;\; \text{sgn}([\hat{\mathbf{q}}]_2)\sqrt{[\hat{\mathbf{q}}_t]_2}\right]^T \quad (20)$$

where sgn($\cdot$) denotes the sign function and $[\hat{\mathbf{q}}_t]_i$ (i=1,2) is the i^{th} element of the third-step estimate. Again, the final estimate is re-inserted into $\mathbf{W}$ and the above procedure is continued until the solution converges. The mixed norm-based MVC IRLS method is summarized in Algorithm 3.

Algorithm 3 Mixed Norm-Based MVC IRLS

1. Obtain the initial position using the LMedS method in the first-step.
2. Construct the diagonal weight matrix employing the initial position obtained from LMedS algorithm as follows:

$$w_i = \begin{cases} \frac{1}{\sigma_1^2 r_i^2} & \text{if } |\frac{r_i - \hat{d}_i}{\sigma_1}| \leq 4.8916; \\ \alpha\left(\frac{\frac{2}{\sigma_{b_i}^2}}{(1+(\frac{e_i^2}{\sigma_{b_i}^2}))^2}\right) & \\ +(1-\alpha)\left(\frac{\frac{1}{\sigma_{b_i}}}{(1+\frac{|e_i|}{\sigma_{b_i}})^2|e_i|}\right), & \text{if } |\frac{r_i - \hat{d}_i}{\sigma_1}| > 4.8916. \end{cases}$$

3. Obtain the second-step WLS estimate.
4. Calculate the third-step WLS estimate using the two-step WLS method.
5. Construct updated weight matrix using the final estimate.

Iterate steps 3-5 until the solution converges. The threshold (4.8916) is determined such that the false alarm probability is set to 10^{-6} in this study, referring to the standard normal table.

C. THE MIXED NORM-BASED UKF WITH LLNCOSH COST CRITERION (MIXED NORM-BASED LLUKF)

The lncosh cost has been widely utilized in the robust adaptive filtering, but has not been employed in the mixed-norm minimization context. The lncosh(e^2) or lncosh($|e|$) cost increases as the magnitude of e increases, thus can be used in the Versoria function by inserting lncosh(e^2) or lncosh($|e|$) into the denominator of the original Versoria function. That is, the following function is obtained:

$$C_{\text{mixed}}(e_{j,k}) = \alpha\left\{\frac{1}{1+\text{lncosh}(\frac{e_{j,k}^2}{\mathbf{P}_{k|k-1}(j,j)})}\right\} + (1-\alpha)\left\{\frac{1}{1+\text{lncosh}(\frac{|e_{j,k}|}{\sqrt{\mathbf{P}_{k|k-1}(j,j)}})}\right\} \quad (21)$$

where $e_{j,k} = \hat{q}_{j,k|k-1} - \hat{q}_{j,k-1|k-1}$ $(j = 1, \cdots, n)$,

$$C_{\text{mixed}}(e_{n+i,k}) = \alpha\left\{\frac{1}{1+\text{lncosh}(\frac{e_{n+i,k}^2}{\sigma_1^2})}\right\} + (1-\alpha)\left\{\frac{1}{1+\text{lncosh}(\frac{|e_{n+i,k}|}{\sigma_1})}\right\} \quad (22)$$

where $e_{n+i,k} = r_i - \hat{r}_{i,k|k-1} - \bar{\mathbf{h}}_{i,k}^T(\hat{\mathbf{q}}_{k|k-1} - \hat{\mathbf{q}}_{k-1|k-1})(i = 1, \cdots, M)$. The mixed-norm-based LLUKF is summarized in Algorithm 4.

D. THE MIXED NORM-BASED IRLS WITH LLNCOSH COST CRITERION (MIXED NORM-BASED LLIRLS)

The mixed norm minimization can be performed using the IRLS method with lncosh cost function. The cost function is defined as follows:

$$J = \frac{1}{2\sigma_{b_i}^2}e_i^2\mathbb{1}(b_i \in \text{LOS}) + \left\{\alpha(\text{lncosh}(\frac{e_i}{\sigma_{b_i}})^2)\right.$$

Algorithm 4 Mixed Norm-Based UKF With Llncosh Criterion (Mixed-Norm LLUKF)

1-7. Identical with Algorithm 1.

8. Utilize the mixed norm-based Versoria function defined as follows:

$\mathbf{C}^{q}_{\text{mixed}} = \text{diag}[C_{\text{mixed}}(e_{1,k}), \cdots, C_{\text{mixed}}(e_{n,k})]$

where $e_{j,k} = \hat{q}_{j,k|k-1} - \hat{q}_{j,k-1|k-1}$.

$$C_{\text{mixed}}(e_{j,k}) = \alpha\left\{\frac{1}{1+\text{lncosh}(A_1)}\right\} + (1-\alpha)\left\{\frac{1}{1+\text{lncosh}(A_2)}\right\}, \quad j=1,\cdots,n$$

where $A_1 = \frac{e^2_{j,k}}{\bar{\mathbf{P}}_{k|k-1}(j,j)}$, $A_2 = \frac{|e_{j,k}|}{\sqrt{\bar{\mathbf{P}}_{k|k-1}(j,j)}}$ and $\alpha \in [0,1]$ is a mixing constant.

$\mathbf{C}^{r}_{\text{mixed}} = \text{diag}[C_{\text{mixed}}(e_{n+1,k}), \cdots, C_{\text{mixed}}(e_{n+M,k})]$

$$C_{\text{mixed}}(e_{n+i,k}) = \alpha\left\{\frac{1}{1+\text{lncosh}(B_1)}\right\} + (1-\alpha)\left\{\frac{1}{1+\text{lncosh}(B_2)}\right\}, \quad i=1,\cdots,M$$

where $B_1 = \frac{e^2_{n+i,k}}{\sigma_1^2}$, $B_2 = \frac{|e_{n+i,k}|}{\sigma_1}$ and $e_{n+i,k} = r_i - \hat{r}_{i,k|k-1} - \bar{\mathbf{h}}^T_{i,k}(\hat{\mathbf{q}}_{k|k-1} - \hat{\mathbf{q}}_{k-1|k-1})$.

$\bar{\mathbf{P}}_{k|k-1} = (\mathbf{C}^{q}_{\text{mixed}})^{-1}$, $\bar{\mathbf{R}}_k = (\mathbf{C}^{r}_{\text{mixed}})^{-1}$

9. Identical with Algorithm 1.

$$+ (1-\alpha)(\text{lncosh}|\frac{e_i}{\sigma_{b_i}}|)\Big\}\mathbb{1}(b_i \in \text{NLOS}) \quad (23)$$

where $\sigma^2_{b_i}$ is the variance of transformed measurement b_i, $e_i = b_i - \mathbf{a}_i^T\mathbf{q}$ and $\mathbf{a}_i^T$ is the i^{th} row of $\mathbf{A}$. Differentiating the cost function with respect to $\mathbf{q}$ yields the following:

$$\frac{\partial J}{\partial \mathbf{q}} = \frac{1}{\sigma^2_{b_i}} e_i \mathbf{a}_i \mathbb{1}(b_i \in \text{LOS}) + \Big\{\alpha\Big(\frac{2e_i}{\sigma^2_{b_i}}\tanh(\frac{e_i^2}{\sigma^2_{b_i}})\Big)\mathbf{a}_i + (1-\alpha)\Big(\frac{e_i}{\sigma_{b_i}|e_i|}\tanh(\frac{|e_i|}{\sigma_{b_i}})\Big)\mathbf{a}_i\Big\}\mathbb{1}(b_i \in \text{NLOS}). \quad (24)$$

Setting the partial derivative to zeros and concatenating each equation yield the following equation:

$$\mathbf{A}^T\mathbf{W}(\mathbf{b} - \mathbf{A}\mathbf{q}) = \mathbf{0} \quad (25)$$

where $\mathbf{W} = \text{diag}[w_1, \cdots, w_M]$, $w_i = \frac{1}{\sigma^2_{b_i}} = \frac{1}{\sigma_1^2 r_i^2}$ if the i^{th} sensor is predicted to be the LOS sensor, $w_i = \alpha\Big(\frac{2}{\sigma^2_{b_i}}\tanh(\frac{e_i^2}{\sigma^2_{b_i}})\Big) + (1-\alpha)\Big(\frac{1}{\sigma_{b_i}|e_i|}\tanh(\frac{|e_i|}{\sigma_{b_i}})\Big)$ if the i^{th} sensor is predicted to be the NLOS sensor. Then, the WLS estimate can be obtained as follows:

$$\hat{\mathbf{q}} = (\mathbf{A}^T\mathbf{W}\mathbf{A})^{-1}\mathbf{A}^T\mathbf{W}\mathbf{b}. \quad (26)$$

The remaining steps are omitted because they are the same as those described in Section IV.B. The mixed norm-based LLIRLS algorithm is summarized in Algorithm 5.

E. ROBUST CLOSED-FORM LOCALIZATION

In this section, the robust closed-form localization is presented. The proposed closed-form localization is composed of three steps. The cost function is defined as follows:

$$J = \frac{1}{2\sigma^2_{b_i}} e_i^2 \mathbb{1}(b_i \in \text{LOS}) + \frac{1}{2\sigma^2_{b_i}} e_i^2 \mathbb{1}(b_i \in \text{NLOS}) \quad (27)$$

where $\sigma^2_{b_i}$ is the variance of transformed observation b_i, $e_i = b_i - \mathbf{a}_i^T\mathbf{q}$ and $\mathbf{a}_i^T$ is the i^{th} row of $\mathbf{A}$. Differentiating the cost function with respect to $\mathbf{q}$ yields the following:

$$\frac{\partial J}{\partial \mathbf{q}} = \frac{1}{\sigma^2_{b_i}} e_i \mathbf{a}_i \mathbb{1}(b_i \in \text{LOS}) + \frac{1}{\sigma^2_{b_i}} e_i \mathbf{a}_i \mathbb{1}(b_i \in \text{NLOS}). \quad (28)$$

Setting the partial derivative to zeros and concatenating each equation yield the following equation:

$$\mathbf{A}^T\mathbf{W}(\mathbf{b} - \mathbf{A}\mathbf{q}) = \mathbf{0} \quad (29)$$

where $\mathbf{W} = \text{diag}[w_1, \cdots, w_M]$, $w_i = \frac{1}{\sigma^2_{b_i}} = \frac{1}{\sigma_1^2 r_i^2}$ if the i^{th} sensor is predicted to be the LOS sensor and $w_i \simeq \frac{1}{(b_i - \hat{b}_i)^2}$ if the corresponding sensor is predicted to be the NLOS sensor. When the sensor is predicted to be in the LOS state, the weight (inverse of the noise variance of the sensor measurement) can be easily computed because the variance of inlier (σ_1^2) is assumed to be known. However, as mentioned earlier, the variance of NLOS sensor observation ($\sigma^2_{b_i}$) is dependent on the unknown measurement bias (μ_2) and outlier noise variance (σ_2^2); thus, the variance of the NLOS transformed observation is estimated using the squared residual [47] in this study. Utilizing this weight matrix, the WLS estimate can be acquired in the second-step and the third-step solution is then obtained via the procedures described in Section IV.B. Clearly, this algorithm has an explicit solution; thus, the proposed closed-form method is advantageous in terms of the divergence problem and computational complexity. The closed-form localization is summarized in Algorithm 6.

Algorithm 5 Mixed Norm-Based IRLS With Llncosh Criterion (Mixed-Norm LLIRLS)

1. Obtain the initial position using the LMedS method in the first-step.

2. Construct the diagonal weight matrix employing the initial position obtained from LMedS algorithm as follows:

$$w_i = \begin{cases} \frac{1}{\sigma_1^2 r_i^2} & \text{if } |\frac{r_i - \hat{d}_i}{\sigma_1}| \le 4.8916; \\ \alpha\Big(\frac{2}{\sigma^2_{b_i}}\tanh(\frac{e_i^2}{\sigma^2_{b_i}})\Big) & \\ +(1-\alpha)\Big(\frac{1}{\sigma_{b_i}|e_i|}\tanh(\frac{|e_i|}{\sigma_{b_i}})\Big), & \text{if } |\frac{r_i - \hat{d}_i}{\sigma_1}| > 4.8916. \end{cases}$$

3. Obtain the second-step WLS estimate.

4. Calculate the third-step WLS estimate using the two-step WLS method.

5. Construct updated weight matrix using the final estimate.

Iterate steps 3-5 until the solution converges.

V. SIMULATION RESULTS

The localization performances of the proposed mixed norm-based UKF and IRLS methods were compared with those of statistical similarity measure (SSM)-based Kalman

Algorithm 6 The Closed-Form Localization

1. Obtain the LMedS estimate in the first-step.
2. Construct the diagonal weight matrix using the LMedS solution as follows:

$$w_i = \begin{cases} \frac{1}{\sigma_1^2 r_i^2} & \text{if } |\frac{r_i - \hat{d}_i}{\sigma_1}| \leq 4.8916; \\ \frac{1}{(b_i - \hat{b}_i)^2}, & \text{if } |\frac{r_i - \hat{d}_i}{\sigma_1}| > 4.8916. \end{cases}$$

3. Obtain the second-step WLS estimate.
4. Calculate the third-step WLS estimate and final estimate using the two-step WLS method.

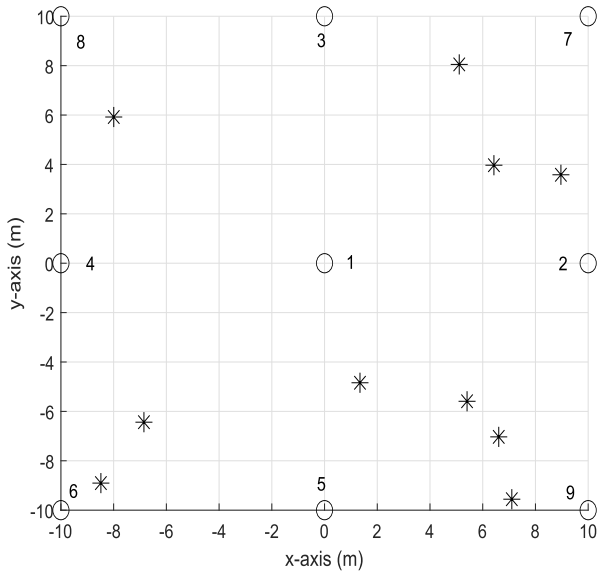

FIGURE 2. Deployment of sensors, where white circles denote sensors and asterisks represent sources.

filter [28], robust EKF [38], and generalized MCC (GMCC) EKF [57] in this section. The SSM Kalman filter employs the SSM vector to quantify the similarity between two vectors, e.g., state vector and predicted state vector. The MCC Kalman filter has been employed to eliminate outliers. However, the Gaussian kernel is not always the best choice. Therefore, the GMCC Kalman filter was investigated to achieve better performance using the generalized Gaussian density function.

A. SIMULATION SETTINGS

The simulation settings are presented in Table 2. Also, the RMSE is defined in (30)

$$\text{RMSE} = \sqrt{\frac{\sum_{i=1}^{10}\sum_{k=1}^{1000}[(\widehat{q_1}^k(i) - q_1(i))^2 + (\widehat{q_2}^k(i) - q_2(i))^2]}{10 \times 1000}} \tag{30}$$

where $[\widehat{q_1}^k(i),\ \widehat{q_2}^k(i)]^T$ is the estimated location of the point target in the i^{th} position set and k^{th} iteration. In addition, $q_1(i)$ and $q_2(i)$ denote the i^{th} true Cartesian coordinates of the emitter. Fig. 2 presents the arrangement of the sensors and the sources, denoted by circles and asterisks, respectively.

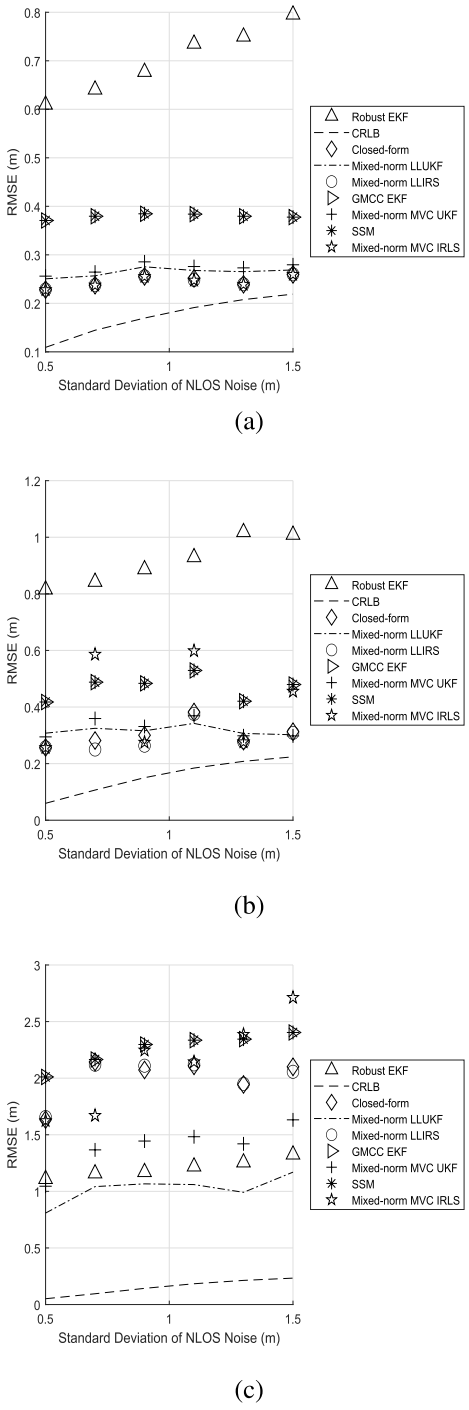

FIGURE 3. Comparison of RMSEs of the proposed estimators with those of existing methods as a function of standard deviation of NLOS noise for different number of NLOS sensors (a) Sensors 8 and 9 are NLOS sensor, measurement bias (μ_2): 5 m, standard deviation of LOS noise (σ_1): 0.3 m (b) Sensors 7, 8 and 9 are NLOS sensor, measurement bias (μ_2): 5 m, standard deviation of LOS noise (σ_1): 0.3 m (c) Sensors 6, 7, 8 and 9 are NLOS sensor, measurement bias (μ_2): 5 m, standard deviation of LOS noise (σ_1): 0.3 m.

B. GENERAL RESULTS

The localization accuracy with respect to the standard deviation of the NLOS error for different number of NLOS sensors was presented in Fig. 3. As shown in Fig. 3(a),

TABLE 2. Simulation settings.

Emitter position	a single emitter located within a 20×20 m^2 region
Number of simulated emitters	10
Number of Monte-Carlo simulation	300
LOS noise variance	assumed to be known and identical
Number of sensors	9
Noise distribution	$N(0,\sigma_1^2)$: LOS state, $N(\mu_2,\sigma_2^2)$: NLOS state
Mixing constant in the mixed norm minimization (α_{mixed})	0.8

sensors 8 and 9 were NLOS sensors and the standard deviation of the LOS noise (σ_1) was 0.3 m. The measurement bias (μ_2) was set to 5 m. The standard deviation of the NLOS noise (σ_2) was set to a larger value than that of the LOS measurement noise [48], [49]. As seen from Fig. 3(a), the RMSEs of the mixed-norm IRLS-based methods were lower than those of the other methods. In Fig. 3(b) and Fig. 3(c), the RMSEs of the proposed mixed-norm UKF-based algorithms were the lowest among the localization methods. Namely, as the number of NLOS sensors increased, the localization performance of the mixed-norm IRLS-based algorithms degraded compared to the other methods. In contrast, the RMSEs of the UKF-based methods were superior to those of the other algorithms as the number of NLOS sensors increased. This demonstrates that the proposed mixed-norm based UKF algorithm was more effective as the number of NLOS sensors increased because the l_1 norm is robust against spurious peaks or impulsive noise. However, the mixed-norm IRLS-based methods were more efficient as the outlyingness (number of NLOS sensors) was lower. As the number of NLOS sensors increased, the localization performance of the mixed-norm IRLS-based methods was degraded because the small noise assumption used in modeling, e.g., neglecting the second-order noise term, was violated. In addition, the proposed mixed-norm LLUKF method outperformed the existing algorithms irrespective of the number of NLOS sensors. As the outlyingness increased, the accuracy of the mixed-norm LLUKF method became higher than those of the other algorithms. Moreover, the RMSEs of the robust localization methods were relatively flat because they were robust against the heavy-tailed noise. The Cramér-Rao lower bound (CRLB) increased as the NLOS noise level increased irrespective of the number of NLOS sensors. The CRLB was calculated using the Monte-Carlo method because the derivation of nonlinear and non-Gaussian distribution is much difficult.

Fig. 4 presents the RMSEs with respect to the standard deviation of LOS noise for different number of NLOS sensors. As shown in Fig. 4(a), sensors 8 and 9 were assumed to be NLOS sensor, whereas the other sensors were LOS sensors. In addition, sensors 7, 8 and 9 were NLOS sensors in Fig. 4(b) and sensors 6, 7, 8 and 9 were NLOS sensors in Fig. 4(c). The RMSEs of all localization methods increased as the standard deviation of LOS noise increased as shown in Fig. 4(a)-(c). The RMSEs of the mixed-norm UKF-based methods were similar to those of the other methods for the low and moderate LOS noise levels; however, the mixed-norm UKF-based algorithms outperformed the other methods in the regimes of large LOS noise. This observation can be explained as follows. As the noise level of LOS observation is larger, the spurious peak or impulsive noise increases. Accordingly, the mixed-norm-based UKF algorithm would be more effective than the other methods because the l_1 norm is robust against spurious peaks. The proposed method has an advantage that the bandwidth is selected as the standard deviation of observation.

Fig. 5 presents the RMSEs with respect to the measurement bias (μ_2) for different number of NLOS sensors. As shown in Fig. 5(a), sensors 8 and 9 were assumed to be NLOS sensor, whereas the other sensors were LOS sensors. In addition, sensors 7, 8 and 9 were NLOS sensors in the Fig. 5(b) and sensors 6, 7, 8 and 9 were NLOS sensors, as shown in Fig. 5(c). As shown in Figs. 5(a)-(c), as the outlyingness increased, the localization performance of the mixed-norm UKF-based method became superior to those of the other algorithms. In Fig. 5(c), the RMSE was larger than the previous results because the contamination ratio approached the breakdown point.

Fig. 6(a) shows the RMSE with respect to the mixing constant (α) when the contamination ratio was low (the number of NLOS sensor was one). The RMSE decreased as the mixing constant approached a unit value because the l_2 norm minimization is more efficient compared to the l_1 norm minimization. Furthermore, Fig. 6(b) illustrates the RMSE in terms of the mixing coefficient when the contamination ratio was moderate (the number of NLOS sensor was four). At this time, the RMSE increased as the mixing constant increased because l_1 norm minimization is robust to the impulsive noise than the l_2 norm minimization. Therefore, the trade-off between small and large mixing constants is required and we determined the mixing constant as 0.8 to assign the larger weight for the l_2 norm minimization because the contamination ratio is usually below 0.5 (i.e., the number of LOS sensor is larger than that of NLOS sensors).

Furthermore, we tested the robustness of the proposed methods for the modeling error. That is, although the measurement noise was modeled as the two-mode Gaussian mixture distribution in this study, the NLOS error

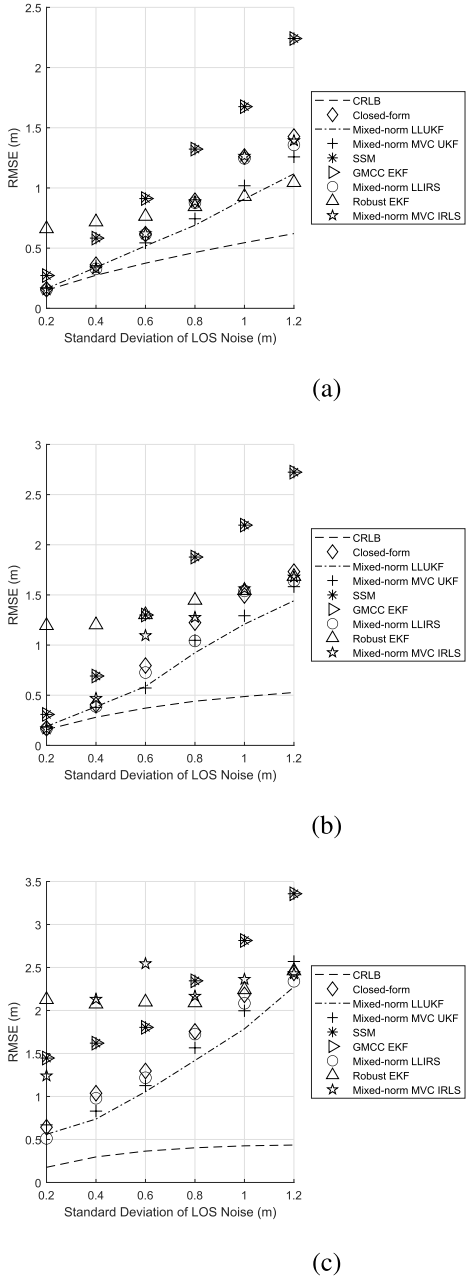

FIGURE 4. Comparison of RMSEs of the proposed estimators with those of existing methods as a function of the standard deviation of LOS noise for different number of NLOS sensors (a) Standard deviation of NLOS noise (σ_2): 1.5 m, measurement bias (μ_2): 5 m, sensors 8 and 9 are NLOS sensors, (b) Standard deviation of NLOS noise (σ_2): 1.5 m, measurement bias (μ_2): 5 m, sensors 7, 8 and 9 are NLOS sensors, (c) Standard deviation of NLOS noise (σ_2): 1.5 m, measurement bias (μ_2): 5 m, sensors 6, 7, 8 and 9 are NLOS sensors.

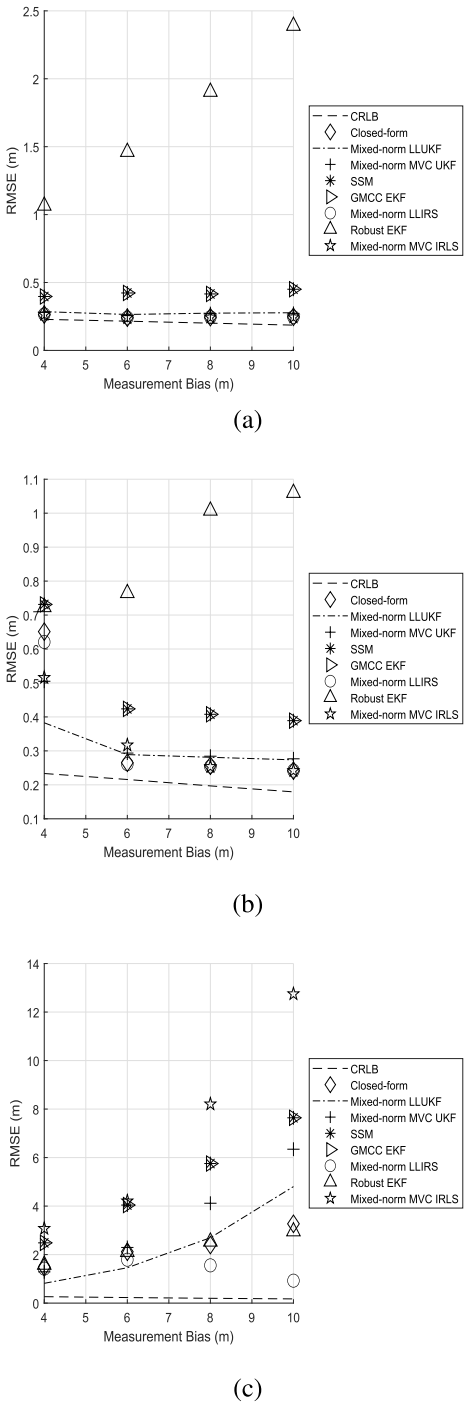

FIGURE 5. Comparison of RMSEs of the proposed estimators with those of existing methods as a function of measurement bias for different number of NLOS sensors (a) Standard deviation of NLOS noise (σ_2): 1.5 m, standard deviation of LOS noise (σ_1): 0.3 m, sensor 8 and 9 are NLOS sensors, (b) Standard deviation of NLOS noise (σ_2): 1.5 m, standard deviation of LOS noise (σ_1): 0.3 m, sensors 7, 8 and 9 are NLOS sensors, (c) Standard deviation of NLOS noise (σ_2): 1.5 m, standard deviation of LOS noise (σ_1): 0.3 m, sensors 6, 7, 8 and 9 are NLOS sensors.

distribution is difficult to be determined accurately. Recently, it was reported that the NLOS error distribution of the ultra-wideband signal follows the heavy-tailed skew-t distribution [58]–[60]. Accordingly, we tested whether the proposed algorithms work effectively against the skew-t NLOS error distribution. Fig. 7 shows the RMSEs with respect to the degree-of-freedom of the skew-t NLOS error distribution. The RMSEs of the proposed UKFs were lower than that of the existing methods because they minimized the l_1/l_2 norms. The RMSEs of all localization methods increased as the degree-of-freedom increased (the

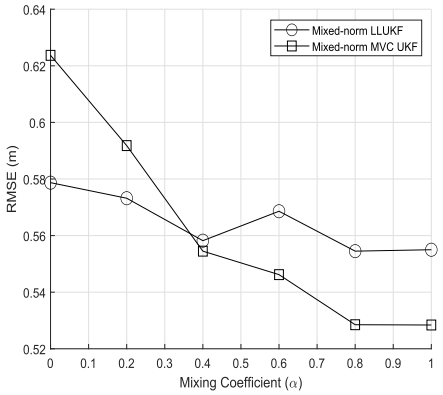

(a)

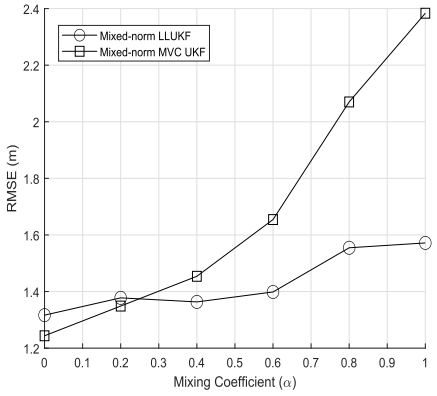

(b)

FIGURE 6. RMSEs of mixed-norm UKFs as a function of the mixing constant (α) (a) Standard deviation of NLOS noise (σ_2): 4 m, standard deviation of LOS noise (σ_1): 0.3 m, μ_2: 5 m, sensor 9 is NLOS sensor, (b) Standard deviation of NLOS noise (σ_2): 4 m, standard deviation of LOS noise (σ_1): 0.3 m, μ_2: 5 m, sensors 6, 7, 8 and 9 are NLOS sensors.

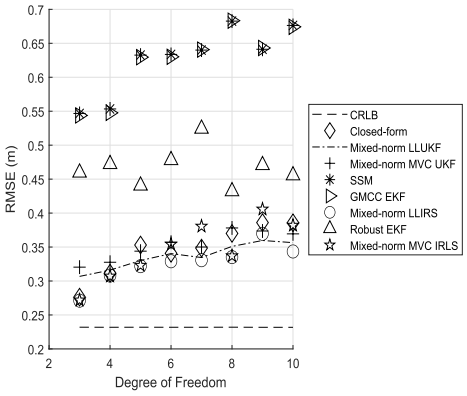

FIGURE 7. RMSEs of localization algorithms as a function of the degree-of-freedom of the skew-t NLOS error distribution (standard deviation of LOS noise (σ_1): 0.3 m, skewness: 2, sensors 6, 7, 8 and 9 are NLOS sensors).

Gaussianity becomes larger, i.e., heavy-tailedness is smaller) because all robust algorithms were designed such that they are more effective in the NLOS conditions compared to the Gaussian distribution-based non-robust algorithms.

Summarizing the above simulation results, the mixed-norm IRLS-based methods were superior to the other methods

TABLE 3. Computational time of localization algorithms.

Method	Computational time (sec)
GMCC EKF	1.9×10^{-3}
Mixed-norm LLUKF	2.6×10^{-3}
Mixed-norm MVC UKF	2.7×10^{-3}
SSM	2.5×10^{-3}
Mixed-norm LLIRS	1.8×10^{-3}
Robust EKF	2.1×10^{-3}
Closed-form	1.6×10^{-3}
Mixed-norm MVC IRLS	1.9×10^{-3}

in the small noise conditions. As the standard deviation of LOS noise increased, the mixed-norm UKFs were moderately superior to the other methods using the convex combination of l_1/l_2 mixed-norm. Also, the mixed-norm UKF methods were robust against the modeling error.

The differences between the proposed methods can be listed as follows:

1) The UKF-based methods are superior to the IRLS-based methods in the low SNR conditions because the IRLS-based methods neglect the second-order noise term. In contrast, the IRLS-based algorithms are slightly superior to the UKF-based algorithms in high SNR conditions.

2) The UKF-based methods do not employ the weight matrix. Instead, the UKF-based method suppresses the adverse effects of outliers using the state error matrix and measurement error matrix that are inversely proportional to the convex combination of the l_1 and l_2 Versoria or lncosh function.

3) The UKF-based method does not utilize the statistical testing to identify the NLOS contaminated sensor unlike the IRLS-based algorithm because the effects of outliers are attenuated automatically using the Versoria or lncosh functions.

4) The closed-form method has an advantage that its computational complexity is low, preserving the moderate estimation performance.

Finally, the computational time was compared. As shown by Table 3, the computational time of IRLS-based methods and closed-form method was smaller than the UKF-based methods. That is, the IRLS-based algorithms and closed-form method were competitive in terms of the localization performance and computational complexity. The computational time of the LMedS method was added because the initial point was computed using the LMedS algorithm.

VI. EXPERIMENT USING THE REAL DATA

In this section, the experimental results using the real data are presented. The real data used in [61] was employed. For details, refer to [61]. Eight sensors were used and their positions were [8.47, 11.87, 0.93] m, [8.41, 7.85, 0.69] m, [5.95, 7.45, 0.64] m, [5.45, 6.71, 1.3] m, [6.95, 0.05, 1.43] m, [2.24, 0.05, 1.47] m, [3.06, 8.33, 1.42] m, [4.47, 11.21, 1.42] m. Also, the source location was [1.55, 3.49, 1.2] m.

TABLE 4. RMSE using real data.

Method	RMSE (m)
GMCC EKF	2.4607
Mixed-norm LLUKF	0.3981
Mixed-norm MVC UKF	0.4267
SSM	3.9802
Mixed-norm LLIRS	0.5948
Robust EKF	3.9795
Closed-form	0.6971
Mixed-norm MVC IRLS	0.5948

Unlike the simulation part, the 3-dimensional localization was performed. Sensors 1, 2, 3 and 4 were NLOS sensors and the remainders were LOS sensors. The trial number of experiments was 30 times and ultra-wideband sensors were used. As seen from Table 4, the localization performances of the UKF-based algorithms were superior to those of other algorithms. Meanwhile, the IRLS-based methods and closed-form algorithm showed the moderate localization performance. The difference between the simulation was that the UKF-based methods used the optimal bandwidth by trial and error to obtain the best performance.

VII. CONCLUSION

Novel robust localization algorithms were developed based on the mixed-norm MVC UKF, mixed-norm LLUKF, mixed-norm LLIRLS, mixed-norm MVC IRLS and closed-form algorithms. The proposed robust mixed-norm UKF-based methods did not require the discrimination of LOS and NLOS sensor. Namely, the mixed-norm-based UKF-based methods did not require statistical testing. The mixed norm UKF-based methods were similar to the other methods in the small inlier noise conditions, but outperformed the other methods in the large LOS noise environments. This observation is caused by the superiority of the l_1 norm minimization against spurious peaks and impulsive noise which increased as the noise level increased. Meanwhile, the proposed mixed-norm IRLS-based algorithms required the statistical testing and were superior to the other methods in the high SNR regimes because it is optimal under a sufficiently small noise conditions. However, the localization performance of the IRLS-based techniques was inferior to that of the other methods in large LOS noise conditions. The IRLS-based methods required a weight matrix and it was obtained inspired by the existing RWGH method. In addition, a closed-form localization algorithm that does not require an initial guess solution and does not have a divergence problem was developed.

REFERENCES

[1] D. Torrieri, "Statistical theory of passive location systems," *IEEE Trans. Aerosp. Electron. Syst.*, vol. AES-20, no. 2, pp. 183–198, Mar. 1983.

[2] Y. T. Chan and K. C. Ho, "A simple and efficient estimator for hyperbolic location," *IEEE Trans. Signal Process.*, vol. 42, no. 8, pp. 1905–1915, Aug. 1994.

[3] H. C. So and L. Lin, "Linear least squares approach for accurate received signal strength based source localization," *IEEE Trans. Signal Process.*, vol. 59, no. 8, pp. 4035–4040, Aug. 2011.

[4] C.-H. Park and J.-H. Chang, "Closed-form localization for distributed MIMO radar systems using time delay measurements," *IEEE Trans. Wireless Commun.*, vol. 15, no. 2, pp. 1480–1490, Feb. 2016.

[5] C.-H. Park and J.-H. Chang, "Shrinkage estimation-based source localization with minimum mean squared error criterion and minimum bias criterion," *Digit. Signal Process.*, vol. 29, pp. 100–106, Jun. 2014.

[6] J. A. Belloch, A. Gonzalez, A. M. Vidal, and M. Cobos, "On the performance of multi-GPU-based expert systems for acoustic localization involving massive microphone arrays," *Expert Syst. Appl.*, vol. 42, no. 13, pp. 5607–5620, Aug. 2015.

[7] S. Zhang, S. Gao, and G. Wang, "Robust NLOS error mitigation method for TOA-based localization via second-order cone relaxation," *IEEE Commun. Lett.*, vol. 19, no. 12, pp. 2210–2213, Dec. 2015.

[8] G. Wang, H. Chen, Y. Li, and N. Ansari, "NLOS error mitigation for TOA-based localization via convex relaxation," *IEEE Trans. Wireless Commun.*, vol. 13, no. 8, pp. 4119–4131, Aug. 2014.

[9] R. M. Vaghefi, J. Schloemann, and R. M. Buehrer, "NLOS mitigation in TOA-based localization using semidefinite programming," in *Proc. IEEE WPNC*, Dresden, Germany, Mar. 2013, pp. 1–6.

[10] R. M. Vaghefi and R. M. Buehrer, "Cooperative localization in NLOS environments using semidefinite programming," *IEEE Commun. Lett.*, vol. 19, no. 8, pp. 1382–1385, Aug. 2015.

[11] S. Tomic and M. Beko, "A bisection-based approach for exact target localization in NLOS environments," *Signal Process.*, vol. 143, pp. 328–335, Feb. 2018.

[12] P. J. Rousseeuw and A. M. Leroy, *Robust Regression and Outlier Detection*. Hoboken, NJ, USA: Wiley, 1987.

[13] Z. Li, W. Trappe, Y. Zhang, and B. Nath, "Robust statistical methods for securing wireless localization in sensor networks," in *Proc. IEEE Int. Symp. Inf. Process. Sensor Netw.*, Los Angeles, CA, USA, Apr. 2005, pp. 91–98.

[14] R. Casas, A. Marco, J. J. Guerrero, and J. Falcó, "Robust estimator for non-line-of-sight error mitigation in indoor localization," *EURASIP J. Adv. Signal Process.*, vol. 2006, no. 1, pp. 1–8, Dec. 2006.

[15] C.-H. Park, S. Lee, and J.-H. Chang, "Robust closed-form time-of-arrival source localization based on α-trimmed mean and Hodges–Lehmann estimator under NLOS environments," *Signal Process.*, vol. 111, pp. 113–123, Jun. 2015.

[16] X.-W. Chang and Y. Guo, "Huber's M-estimation in relative GPS positioning: Computational aspects," *J. Geodesy*, vol. 79, nos. 6–7, pp. 351–362, Aug. 2005.

[17] J. L. Hodges and E. L. Lehmann, "Estimates of location based on rank tests," *Ann. Math. Stat.*, vol. 34, no. 2, pp. 598–611, 1963.

[18] I. Guvenc, C.-C. Chong, and F. Watanabe, "NLOS identification and mitigation for UWB localization systems," in *Proc. IEEE WCNC*, Hong Kong, Mar. 2007, pp. 1571–1576.

[19] Y.-T. Chan, W.-Y. Tsui, H.-C. So, and P.-C. Ching, "Time-of-arrival based localization under NLOS conditions," *IEEE Trans. Veh. Technol.*, vol. 55, no. 1, pp. 17–24, Jan. 2006.

[20] C.-H. Park and J.-H. Chang, "Robust time-of-arrival source localization employing error covariance of sample mean and sample median in line-of-sight/non-line-of-sight mixture environments," *EURASIP J. Adv. Signal Process.*, vol. 2016, p. 89, Dec. 2016.

[21] S. Gezici, H. Kobayashi, and H. V. Poor, "Nonparametric nonline-of-sight identification," in *Proc. IEEE Veh. Technol. Conf.*, Orlando, FL, USA, Mar. 2003, pp. 2544–2548.

[22] B. Chen, X. Liu, H. Zhao, and J. C. Principe, "Maximum correntropy Kalman filter," *Automatica*, vol. 76, pp. 70–77, Feb. 2017.

[23] X. Liu, H. Qu, J. Zhao, P. Yue, and M. Wang, "Maximum correntropy unscented Kalman filter for spacecraft relative state estimation," *Sensors*, vol. 16, no. 9, pp. 1–16, Sep. 2016.

[24] C. Liu and M. Jiang, "Robust adaptive filter with lncosh cost," *Signal Process.*, vol. 168, pp. 1–14, Mar. 2020.

[25] U. Hammes and A. M. Zoubir, "Robust MT tracking based on M-estimation and interacting multiple model algorithm," *IEEE Trans. Signal Process.*, vol. 59, no. 7, pp. 3398–3409, Jul. 2011.

[26] Y. Huang, Y. Zhang, N. Li, Z. Wu, and J. A. Chambers, "A novel robust Student's t-based Kalman filter," *IEEE Trans. Aerosp. Electron. Syst.*, vol. 53, no. 3, pp. 1545–1554, Jun. 2017.

[27] Y. Huang, Y. Zhang, Y. Zhao, and J. A. Chambers, "A novel robust Gaussian–Student's t mixture distribution based Kalman filter," *IEEE Trans. Signal Process.*, vol. 67, no. 13, pp. 3606–3620, Jul. 2019.
[28] Y. Huang, Y. Zhang, Y. Zhao, P. Shi, and J. A. Chambers, "A novel outlier-robust Kalman filtering framework based on statistical similarity measure," *IEEE Trans. Autom. Control*, vol. 66, no. 6, pp. 2677–2692, Jun. 2020.
[29] S.-I. Sou, F.-J. Wu, and W.-C. Wu, "JoLo: Multi-device joint localization based on wireless data fusion," *IEEE Trans. Mobile Comput.*, early access, Feb. 14, 2022, doi: 10.1109/TMC.2022.3150758.
[30] S. Kumar and S. K. Das, "Target detection and localization methods using compartmental model for Internet of Things," *IEEE Trans. Mobile Comput.*, vol. 19, no. 9, pp. 2234–2249, Sep. 2020.
[31] T.-J. Ho, M.-H. Wu, and W.-C. Lin, "Mobile localization in random NLOS settings using improved particle filtering," in *Proc. 13th Int. Congr. Ultra Modern Telecommun. Control Syst. Workshops (ICUMT)*, Brno, Czech Republic, Oct. 2021, pp. 44–49.
[32] Y. Huang, S. Mazuelas, F. Ge, and Y. Shen, "Indoor localization system with NLOS mitigation based on self-training," *IEEE Trans. Mobile Comput.*, early access, Feb. 4, 2022, doi: 10.1109/TMC.2022.3148338.
[33] S. Zhao, N. Guo, X.-P. Zhang, X. Cui, and M. Lu, "Sequential Doppler shift based optimal localization and synchronization with TOA," *IEEE Internet Things J.*, early access, Feb. 10, 2022, doi: 10.1109/JIOT.2022.3150564.
[34] M. Katwe, P. Ghare, and P. K. Sharma, "Robust NLOS bias mitigation for hybrid RSS-TOA based source localization under unknown transmission parameters," *IEEE Wireless Commun. Lett.*, vol. 10, no. 3, pp. 542–546, Mar. 2021.
[35] K. Panwar, M. Katwe, P. Babu, P. Ghare, and K. Singh, "A majorization-minimization algorithm for hybrid TOA-RSS based localization in NLOS environment," *IEEE Commun. Lett.*, vol. 26, no. 5, pp. 1017–1021, May 2022, doi: 10.1109/LCOMM.2022.3155685.
[36] P. Zuo, H. Zhang, C. Wang, H. Jiang, and B. Pan, "Directional target localization in NLOS environments using RSS-TOA combined measurements," *IEEE Wireless Commun. Lett.*, vol. 10, no. 11, pp. 2602–2606, Nov. 2021.
[37] C. E. O'Lone, H. S. Dhillon, and R. M. Buehrer, "Characterizing the first-arriving multipath component in 5G millimeter wave networks: TOA, AOA, and non-line-of-sight bias," *IEEE Trans. Wireless Commun.*, vol. 21, no. 3, pp. 1602–1620, Mar. 2022.
[38] S. K. Das and R. Mudi, "Kalman filter based NLOS identification and mitigation for M2M communications over cellular networks," in *Proc. IEEE 93rd Veh. Technol. Conf. (VTC-Spring)*, Apr. 2021, pp. 1–6.
[39] F. Huang, J. Zhang, and S. Zhang, "Maximum versoria criterion-based robust adaptive filtering algorithm," *IEEE Trans. Circuits Syst. II, Exp. Briefs*, vol. 64, no. 10, pp. 1252–1256, Oct. 2017.
[40] C. Shen and L. Mihaylova, "A flexible robust Student's t-based multimodel approach with maximum versoria criterion," *Signal Process.*, vol. 182, May 2021, Art. no. 107941.
[41] C.-H. Park and J.-H. Chang, "Robust localization employing weighted least squares method based on MM estimator and Kalman filter with maximum versoria criterion," *IEEE Signal Process. Lett.*, vol. 28, pp. 1075–1079, May 2021.
[42] J. Chambers and A. Avlonitis, "A robust mixed-norm adaptive filter algorithm," *IEEE Signal Process. Lett.*, vol. 4, no. 2, pp. 46–48, Feb. 1997.
[43] X. Songlei, W. Yibo, S. Zhen, and C. Xu, "Internal multiple adaptive subtraction using Huber norm," *J. Appl. Geophys.*, vol. 116, pp. 104–109, May 2015.
[44] R. R. Wilcox, *Introduction to Robust Estimation and Hypothesis Testing*, 3rd ed. New York, NY, USA: Academic, 2012.
[45] R. A. Maronna, D. R. Martin, and V. J. Yohai, *Robust Statistics: Theory and Methods*. Hoboken, NJ, USA: Wiley, 2006.
[46] P. J. Huber and E. M. Ronchetti, *Robust Statistics*. Hoboken, NJ, USA: Wiley, 2009.
[47] P.-C. Chen, "A non-line-of-sight error mitigation algorithm in location estimation," in *Proc. Wireless Commun. Netw. Conf.*, Piscataway, NJ, USA, 1999, pp. 316–320.
[48] F. Yin, C. Fritsche, F. Gustafsson, and A. M. Zoubir, "EM- and JMAP-ML based joint estimation algorithms for robust wireless geolocation in mixed LOS/NLOS environments," *IEEE Trans. Signal Process.*, vol. 62, no. 1, pp. 168–182, Jan. 2014.
[49] Y. Feng, C. Fritsche, F. Gustafsson, and A. M. Zoubir, "TOA-based robust wireless geolocation and Cramér-Rao lower bound analysis in harsh LOS/NLOS environments," *IEEE Trans. Signal Process.*, vol. 61, no. 9, pp. 168–182, May 2013.
[50] F. Gustafsson and F. Gunnarsson, "Mobile positioning using wireless networks," *IEEE Signal Process. Mag.*, vol. 22, no. 4, pp. 41–53, Jul. 2005.
[51] U. Hammes, E. Wolsztynski, and A. M. Zoubir, "Robust tracking and geolocation for wireless networks in NLOS environments," *IEEE J. Selected Top. Signal Process.*, vol. 3, no. 5, pp. 889–901, Oct. 2009.
[52] Y. Susanti, H. Pratiwi, S. Sulistijowati H., and T. Liana, "M estimation, S estimation, and MM estimation in robust regression," *Int. J. Pure Apllied Math.*, vol. 91, no. 3, pp. 349–360, Mar. 2014.
[53] C. H. Park and J.-H. Chang, "Robust localization based on ML-type, multi-stage ML-type, and extrapolated single propagation UKF methods under mixed LOS/NLOS conditions," *IEEE Trans. Wireless Commun.*, vol. 19, no. 9, pp. 5819–5832, Sep. 2020.
[54] G. Wang, N. Li, and Y. Zhang, "Maximum correntropy unscented Kalman and information filters for non-Gaussian measurement noise," *J. Franklin Inst.*, vol. 354, no. 18, pp. 8659–8677, Oct. 2017.
[55] S. J. Julier and J. K. Uhlmann, "Unscented filtering and nonlinear estimation," *Proc. IEEE*, vol. 92, no. 3, pp. 401–422, Mar. 2004.
[56] S. J. Julier, "The spherical simplex unscented transformation," in *Proc. Amer. Control Conf.*, Denver, CO, USA, Jun. 2003, pp. 2430–2434.
[57] F. Ma, J. He, and X. Zhang, "Robust Kalman filter algorithm based on generalized correntropy for ultra-wideband ranging in industrial environment," *IEEE Access*, vol. 7, pp. 27490–27500, 2019.
[58] J. V. Valls and P. Closas, "NLOS mitigation in indoor localization by marginalized Monte Carlo Gaussian smoothing," *Eurasip J. Adv. Signal Process.*, vol. 2017, p. 62, Dec. 2017.
[59] H. Nurminen, T. Ardeshiri, R. Piche, and F. Gustafsson, "Robust inference for state-space models with skewed measurement noise," *IEEE Signal Process. Lett.*, vol. 22, no. 11, pp. 1898–1902, Nov. 2015.
[60] G. Miraglia, K. N. Maleki, and L. R. Hook, "Comparison of two sensor data fusion methods in a tightly coupled UWB/IMU 3-D localization system," in *Proc. Int. Conf. Eng., Technol. Innov. (ICE/ITMC)*, Jun. 2017, pp. 611–618.
[61] K. Bregar and M. Mohorčič, "Improving indoor localization using convolutional neural networks on computationally restricted devices," *IEEE Access*, vol. 6, pp. 17429–17441, 2018.

CHEE-HYUN PARK received the Ph.D. degree in electronics and computer engineering from Sungkyunkwan University, Suwon, South Korea, in 2011. From April 2011 to August 2012, he was a Postdoctoral Fellow with the University of Wisconsin–Madison, Madison, WI, USA. He is currently a Research Professor with Hanyang University, Seoul, South Korea. His research interests include detection and estimation theory, source localization, array signal processing, and machine learning.

JOON-HYUK CHANG (Senior Member, IEEE) received the B.S. degree in electronics engineering from Kyungpook National University, Daegu, South Korea, in 1998, and the M.S. and Ph.D. degrees in electrical engineering from Seoul National University, South Korea, in 2000 and 2004, respectively. From 2000 to 2005, he was a Chief Engineer with Netdus Corporation, Seoul, South Korea. From 2004 to 2005, he held a post-doctoral position with the University of California at Santa Barbara, Santa Barbara, CA, USA, where he was involved in adaptive signal processing and audio coding. In 2005, he joined the Korea Institute of Science and Technology, Seoul, as a Research Scientist, where he was involved in speech recognition. From 2005 to 2011, he was an Assistant Professor with the School of Electronic Engineering, Inha University, Incheon, South Korea. He is currently a Full Professor with the School of Electronic Engineering, Hanyang University, Seoul. His research interests include speech coding, speech enhancement, speech recognition, audio coding, and adaptive signal processing. He was recipient of the IEEE/IEEK IT Young Engineer of the year 2011. He is serving as the Editor-in-Chief for the Signal Processing Society Journal of the IEEK.